On the initial stage of the evolution of hydrodynamic parameters during deep penetration of metals by high-power laser radiation

© R.D. Seidgazov, F.Kh. Mirzade

Institute on Laser and Information Technologies Branch of the Federal Scientific Research Center ‚Crystallography and Photonics", Russian Academy of Sciences, Shatura, Moscow region, Russia
E-mail: seidgazov@mail.ru

A qualitative analysis of changes in hydrodynamic parameters during keyhole formation by thermocapillary melt removal under the point action of CW laser radiation is presented. It is established that rapid surface deformation leads to adhesion of the viscous sublayer to the melting boundary and creation the shear structure of thermocapillary flow which stimulates acceleration of keyhole growth.

Keywords: keyhole formation, laser radiation, thermocapillary effect, shear flow, viscous sublayer, sticking.

The keyhole mode ensures substantial penetration depth and productivity in laser welding and additive manufacturing by Laser Powder Bed Fusion. A transition from conduction to keyhole mode turns the initial shallow and hemispherical melting zone into a deep and narrow one due to the keyhole formation along which laser beam penetrates deep into the metal. Two hydrodynamic mechanisms (ablation and thermocapillary (TC)) may be involved in the formation of this keyhole, but opinions regarding the relative influence of these mechanisms differ. The ablation mechanism sustains a keyhole mechanically by the vapor recoil pressure [1,2] and is traditionally considered to be the dominant one. A threshold change of melting regimes is assumed to be the result of a sharp increase in vapor pressure occurring when the surface temperature reaches boiling point T_B [3]. It should be noted that the use of the ablation mechanism is sometimes accompanied by confessions of researchers about their lack of adequate knowledge about the mechanism of deep penetration [4–6].

The other mechanism of deep penetration is related to the TC mechanism of removal of molten metal due to the temperature dependence of surface tension under nonuniform laser heating, which allows one to control the keyhole formation [7,8]. The results of thorough numerical calculations of the crater formation with the relative influence of both mechanisms taken into account [9] confirmed that the TC mechanism is dominant at boiling point T_B and that the ablation mechanism becomes dominant only at significantly higher temperatures. The evaporation rate in the keyhole mode (or at surface temperature T_B [3]) is insufficient to sustain a keyhole mechanically by the vapor pressure, and the experimental data for this regime are reproducible in evaluation calculations relying on the TC mechanism [10–12]. Estimates of the keyhole mode threshold for the TC mechanism agree with the results of experiments which used different metals in a wide range

of variation of process parameters [13]. Thus, the weight of evidence suggests that the TC mechanism plays a major role here, although one should still present a solid argument for the emergence of a shear TC flow in metals at low Prandtl numbers ($\mathrm{Pr} = \nu/\chi \ll 1$, ν is the kinematic viscosity and χ is the thermal diffusivity) that are typical of them. In order to do this, one needs to analyze from a physical standpoint the evolution of process parameters at the initial stage of laser melting under the influence of the TC mechanism. The aim of the present study is to perform this analysis for point melting with the use of approximate dependences.

Let us consider the initial moment of point metal melting by continuous laser radiation with diameter d and analyze the formation of a shear TC flow before the keyhole is formed (Fig. 1). With this end in view, let us examine the evolution of the surface temperature, the TC flow velocity, the melting front and surface deformation speed, the thickness of the molten layer and the viscous sublayer, and the penetration and keyhole depth under constant metal properties.

Melt temperature. Laser radiation is absorbed within a very thin layer on the metal surface. Distance x of propagation of a heat wave within time t is estimated roughly as $x(t) = (\chi t)^{1/2}$ [14]. The surface temperature variation under the influence of a surface heat source ($\alpha^{-1} \ll (\chi t)^{1/2}$, α is the absorption coefficient) with a constant absorbed power density q is [14]

$$\Delta T(t) = (2q/\lambda)(\chi t/\pi)^{1/2},$$

where λ is the thermal conductivity. If λ and χ are assumed to be constants, the temperature grows as $\Delta T(t) \sim t^{1/2}$. The process of melting commences at temperature T_M and time point t_M. At the time of t_B, the temperature saturates at boiling point T_B [3]. Therefore, two intervals may be identified in the melting process: $t_M < t < t_B$ with
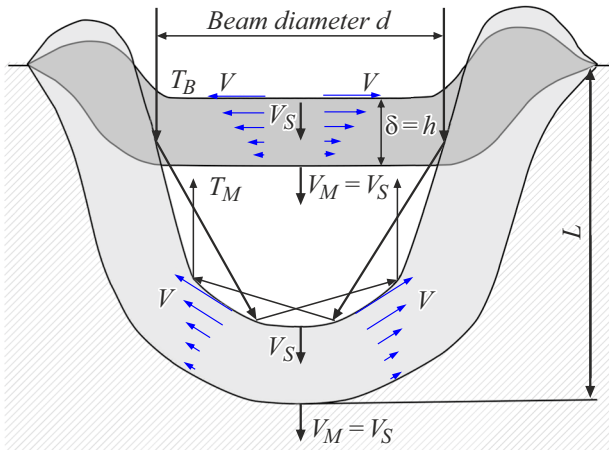
Figure 1. Laser melt removal by a thermocapillary shear flow and crater growth in the steady-state regime at $h(t) = \delta(t)$ and $V_S(t) = V_M(t)$ with radiation capture.

temperature $T(t) \sim t^{1/2}$ and $t > t_B$ where the temperature reaches saturation $T(t) = T_B$ (Fig. 2, a).

Viscous sublayer thickness. With the emergence of a TC flow, viscous forces are transferred to the lower layers and extend over a distance of thickness δ of the viscous sublayer similarly to the temperature propagation $\delta(t) = (\nu t)^{1/2}$ [7,8] (Fig. 2, c). This growth of $\delta(t)$ is maintained for as long as the TC flow is present.

Thermocapillary flow velocity. The TC flow velocity increases from the moment of t_M as $V(t) \approx \sigma_T \big(T(t) - T_M\big)\delta(t)/(\eta d)$ [7,8], where σ_T is the temperature coefficient of surface tension and η is the dynamic viscosity. The TC flow velocity in the $t_M < t < t_B$ interval increases linearly with time $V(t) \sim \big(T(t) - T_M T\big)\delta(t) \sim t$. At $t > t_B$ with the temperature saturated ($T(t) = T_B$), the flow velocity grows with a nonlinear slowdown in time $V(t) \sim T_B \delta(t) \sim t^{1/2}$ (Fig. 2, a).

Surface deformation speed . The radial spread of the TC flow with velocity V at thickness δ of the viscous sublayer induces melt surface deformation with speed $V_S(t)$ (Fig. 1) in the irradiated zone. It follows from mass conservation condition $V_S(t)\pi d^2/4 = V(t)\delta(t)\pi d$ that $V_S(t) = 4V(t)\delta(t)/d$. At $V(t) \sim t$ and $\delta(t) \sim t^{1/2}$, the surface deformation first ($t_M < t < t_B$) spreads with a nonlinear acceleration $V_S(t) \sim t^{3/2}$; following the saturation of temperature (at $t > t_B$), this spread then slows down due to $V(t) \sim t^{1/2}$ and $\delta(t) \sim t^{1/2}$ and assumes a linear nature: $V_S(t) \sim t$ (Fig. 2, b).

Molten layer thickness. Molten layer thickness $h(t)$ is defined by the movement of two phase boundaries. Thickness $h(t)$ in a moving system of reference tied to the absorbing surface increases with penetration of the melting front deeper into the metal with speed $V_M(t) \approx (\chi/t)^{1/2}$ and decreases as the solid metal material is supplied to the
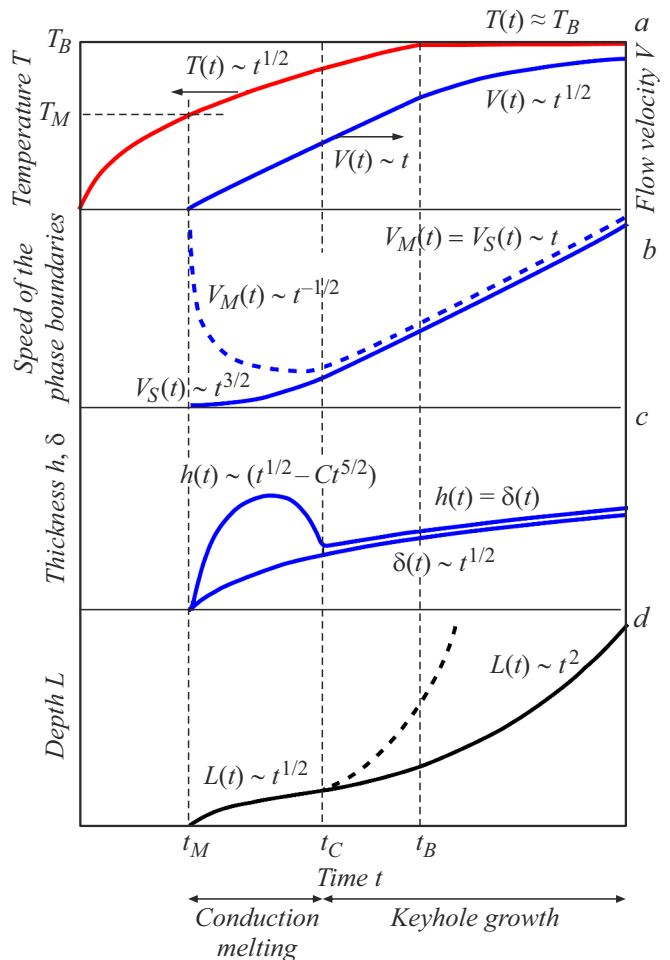
melting front with surface deformation speed $V_S(t)$:

$$h(t) = \big[V_M(t) - V_S(t)\big]t.$$

Using the relations for $V_M(t)$, $V_S(t)$, $T(t)$ and introducing notation $C = 8q\nu/(\pi^{1/2}d\lambda)$, we obtain

$$h(t) = \chi^{1/2}(t^{1/2} - Ct^{5/2}).$$

At the onset of melting, the rapid growth of $h(t)$ is governed by thermal conductivity: $h(t) \sim t^{1/2}$. The melting front speed decreases with time from its maximum value of $V_M(t_M)$ with a nonlinear slowdown $V_M(t) \sim t^{-1/2}$, while the deformation speed increases from zero $V_S(t_M) = 0$ with a nonlinear acceleration $V_S(t) \sim t^{3/2}$. Thickness $h(t)$ grows until the speeds of phase boundaries become equal. After that, thickness $h(t)$ decreases under the influence of acceleration of surface deformation $V_S(t) \sim t^{3/2}$ up to the time point (t_C) of sticking of the viscous sublayer to melting boundary and the formation of a shear TC flow structure: $h(t) = \delta(t)$ (Figs. 1 and 2, c). From

Figure 2. Evolution of parameters governing the penetration of metals. a — surface temperature $T(t)$, TC flow velocity $V(t)$; b — melt front speed $V_M(t)$, surface deformation speed $V_S(t)$; c — molten layer thickness $h(t)$, viscous sublayer thickness $\delta(t)$; d — penetration depth $L(t)$.

that point on $(t > t_C)$, the heat source on an accelerating free surface facilitates the melting front acceleration by an enhancement of heat transfer due to convective heat transport in the viscous sublayer. Thus, thickness $h(t)$ increases together with viscous sublayer thickness $h(t) = \delta(t) \sim t^{1/2}$ at equal velocities $V_M(t) = V_S(t)$ and with the TC flow assuming a shear structure. The rapid keyhole growth in the steady-state regime, which was characterized theoretically in [7,8], provides for efficient removal of melt from the irradiated region. Sticking condition $h(t) = \delta(t)$ is violated when the limiting keyhole depth is reached and the process of melt removal from the keyhole stops under continuous melting by laser radiation.

Penetration depth. The moment of sticking t_C divides the melting process into two phases: the phase of preparation of a shear TC flow $(t_M < t < t_C)$ and the phase of steady-state keyhole growth $(t > t_C)$ (Fig. 2, *d*). The first one is characterized by an insignificant surface deformation with an increase in penetration depth due to thermal conductivity: $L(t) \approx h(t) \sim (\chi t)^{1/2} \sim t^{1/2}$. The second phase involves the keyhole growth and nonlinear acceleration of penetration: $L(t) \approx V_S(t)t \sim T(t)\delta^2(t)t \sim t^{5/2}$ at $t_M < t < t_C$ and $L(t) \approx T_B \delta^2(t)t \sim t^2$ at $t > t_C$. An absorption jump resulting from radiation capture by a cavern (Fig. 1) accelerates the keyhole growth additionally (dashed curve in Fig. 2, *d*) [15]. The existence of two melting phases with a characteristic bend of evolution curve $L(t)$ is confirmed in observations (with high-speed X-ray visualization) of keyhole growth in metal [16]. According to the obtained data, the duration of the first phase decreases as the radiation power grows (and as the laser spot diameter decreases).

Thus, regardless of the fact that metals typically have very low Prandtl numbers ($Pr = \nu/\chi \ll 1$), rapid surface deformation in keyhole mode is conducive to the short-term emergence of a shear flow at the melting front. The moment of sticking is distinguished by a bend in evolution curve $L(t)$ and divides the process of laser melting in keyhole mode into the phase of preparation of a shear flow and the phase of steady-state keyhole growth. When the keyhole reaches its ultimate depth, the surface deformation ceases. The thickness of the molten layer starts increasing from this moment, and the viscous sublayer gets detached from the melting boundary (the sticking condition is violated). A convective TC flow with a near-wall backward flow forms, and a crater thus gets filled and vanishes, although the exposure to laser radiation remains uninterrupted. This was demonstrated experimentally in [12].

The hydrodynamic processes described above are microscopic in scale. At thickness $h = \delta \sim 5-10\,\mu$m and TC flow velocity $V \sim 5-10$ m/s, the characteristic propagation time of viscous forces is $\delta/V \sim 1\,\mu$s [8]. An even finer spatiotemporal grid and substantial computational resources are needed to model numerically the TC keyhole formation. The disregard of these requirements in calculations may translate into erroneous results and conclusions regarding the role of the TC mechanism.

Conflict of interest

The authors declare that they have no conflict of interest.

References

[1] M.S. Baranov, B.A. Vershok, I.N. Geinrikhs, High Temp., **13** (3), 515 (1975).

[2] J.G. Andrews, D.R. Atthey, J. Phys. D: Appl. Phys., **9** (15), 2181 (1976). DOI: 10.1088/0022-3727/9/15/009

[3] K. Hirano, R. Fabbro, M. Muller, J. Phys. D: Appl. Phys., **44** (43), 435402 (2011). DOI: 10.1088/0022-3727/44/43/435402

[4] T. DebRoy, S.A. David, Rev. Mod. Phys., **67** (1), 85 (1995). DOI: 10.1103/RevModPhys.67.85

[5] R. Fabbro, M. Hamadou, F. Coste, J. Laser Appl., **16** (1), 16 (2004). DOI: 10.2351/1.1642633

[6] M. Courtois, M. Carin, P. Le Masson, S. Gaied, M. Balabane, J. Phys. D: Appl. Phys., **49** (15), 155503 (2016). DOI: 10.1088/0022-3727/49/15/155503

[7] R.D. Seidgazov, Yu.M. Senatorov, Sov. J. Quantum Electron., **18** (3), 396 (1988). DOI: 10.1070/QE1988v018n03ABEH011530.

[8] R.D. Seidgazov, J. Phys. D: Appl. Phys., **42** (17), 175501 (2009). DOI: 10.1088/0022-3727/42/17/175501

[9] S. Ly, G. Guss, A.M. Rubenchik, W.J. Keller, N. Shen, R.A. Negres, J. Bude, Sci. Rep., **9**, 8152 (2019). DOI: 10.1038/s41598-019-44577-6

[10] R.D. Seidgazov, in *Proc. of the Forth Int. Conf. „Laser technologies in welding and material processing"*(E.O. Paton Electric Welding Institute NASU, Kyiv, 2009), p. 62. DOI: 10.13140/RG.2.1.1247.3767

[11] R.D. Seidgazov, in *2019 IEEE 8th Int. Conf. on advanced optoelectronics and lasers (CAOL)* (Sozopol, Bulgaria, 2019), p. 216. DOI: 10.1109/CAOL46282.2019.9019431

[12] R.D. Seidgazov, F.Kh. Mirzade, Pis'ma Zh. Tekh. Fiz., **47** (21), 16 (2021) (in Russian). DOI: 10.21883/PJTF.2021.21.51622.18838

[13] R.D. Seidgazov, F.Kh. Mirzade, Welding Int., **35** (7-9), 359 (2021). DOI: 10.1080/09507116.2021.1979829

[14] W.W. Duley, *Laser processing and analysis of materials* (Plenum Press, N.Y.−London, 1983). DOI: 10.1007/978-1-4757-0193-7

[15] R. Fabbro, Appl. Sci., **10** (4), 1487 (2020). DOI: 10.3390/app10041487

[16] R. Cunningham, C. Zhao, N. Parab, C. Kantzos, J. Pauza, K. Fezzaa, T. Sun, A.D. Rollett, Science, **363** (6429), 849 (2019). DOI: 10.1126/science.aav4687